

Multifractal statistics of the local order parameter at random critical points: Application to wetting transitions with disorder

Cécile Monthus and Thomas Garel

Service de Physique Théorique, CEA/DSM/SPHT, Unité de recherche associée au CNRS, 91191 Gif-sur-Yvette cedex, France

(Received 3 May 2007; published 21 August 2007)

Disordered systems present multifractal properties at criticality. In particular, as discovered by Ludwig [A.W.W. Ludwig, Nucl. Phys. B **330**, 639 (1990)] in the case of a diluted two-dimensional Potts model, the moments $\overline{\rho^q(r)}$ of the local order parameter $\rho(r)$ scale with a set $x(q)$ of nontrivial exponents $x(q) \neq qx(1)$. We reexamine these ideas to incorporate more recent findings: (i) whenever a multifractal measure $w(r)$ normalized over space $\sum_r w(r)=1$ occurs in a random system, it is crucial to distinguish between the typical values and the disorder-averaged values of the generalized moments $Y_q = \sum_r w^q(r)$, since they may scale with different generalized dimensions $D(q)$ and $\tilde{D}(q)$, and (ii), as discovered by Wiseman and Domany [S. Wiseman and E. Domany, Phys. Rev. E **52**, 3469 (1995)], the presence of an infinite correlation length induces a lack of self-averaging at critical points for thermodynamic observables, in particular for the order parameter. After this general discussion, valid for any random critical point, we apply these ideas to random polymer models that can be studied numerically for large sizes and good statistics over the samples. We study the bidimensional wetting or the Poland-Scheraga DNA model with loop exponents $c=1.5$ (marginal disorder) and $c=1.75$ (relevant disorder). Finally, we argue that the presence of finite Griffiths-ordered clusters at criticality determines the asymptotic value $x(q \rightarrow \infty)=d$ and the minimal value $\alpha_{min}=D(q \rightarrow \infty)=d-x(1)$ of the typical multifractal spectrum $f(\alpha)$.

DOI: [10.1103/PhysRevE.76.021114](https://doi.org/10.1103/PhysRevE.76.021114)

PACS number(s): 02.50.-r, 05.40.-a, 05.45.Df

I. INTRODUCTION

Among the various areas where multifractality occurs (see, for instance, [1–7] and references therein), the case of critical points in the presence of frozen disorder is of particular interest. The idea that multifractality occurs at criticality was first established for quantum Anderson localization transitions [8,9] and has been the subject of very detailed studies [10–12]. For the directed polymer in a random medium in dimension 1+3, where a disorder-induced localization-delocalization process occurs, the multifractal properties studied recently [13] are very similar to the case of Anderson transitions. In the field of spin models, the most studied case seems to be the two-dimensional diluted q -state Potts model, where multifractality was discovered by Ludwig [14] via conformal field theory using perturbation theory in the parameter $(q-2)$ governing the disorder relevance. This work has motivated numerical studies for various values of q [15–18]. The idea of multifractality has been also proposed in other disordered models like spin glasses and random-field spin systems [19–21] and has been studied numerically for spin glasses on diamond hierarchical lattices [22]. Finally, for disordered quantum spin chains, it turns out that the statistics of critical correlation functions is described by “multiscaling,” which is even stronger than multifractality [23]. This is because these disordered quantum spin chains are actually governed by “infinite-disorder fixed points” [24].

So the presence of multifractality at criticality seems generic in disordered systems. However, following [14], most studies of classical disordered models have focused on the statistics of two-point correlation functions, whereas multifractality already occurs at the level of one-point functions like the order parameter or the energy density [14]. In particular, the moments of the local order parameter scale with a

set $x(n)$ of nontrivial exponents $x(n) \neq nx(1)$. In this paper, we reexamine these ideas in the light of more recent findings concerning the possible differences between the exponents for typical and averaged values and the lack of self-averaging of thermodynamic observables at criticality [25–27]. We then study the multifractal statistics of the order parameter in random polymer models that can be studied numerically for large sizes and good statistics over the samples.

The paper is organized as follows. In Sec. II, we summarize the outcome of previous works concerning the multifractal statistics and the lack of self-averaging at random critical points. In the remainder of the paper, we apply these ideas to wetting transitions with disorder. These random polymer models are presented in Sec. III. Our numerical results on the statistics of the local order parameter are given, respectively, in Sec. IV for loop exponent $c=1.75$ (relevant disorder) and in Sec. V for loop exponent $c=1.5$ (marginal disorder). In Sec. VI, we discuss the influence of boundary conditions on the multifractal spectrum. Section VII contains our conclusions.

II. MULTIFRACTAL STATISTICS OF THE LOCAL ORDER PARAMETER AT CRITICALITY

A. Disorder-averaged moments of the local order parameter

Let $\rho(r; i, L)$ be the local order parameter at site r in a finite disordered sample i of volume L^d in dimension d . This local order parameter is usually defined in terms of a thermal average: for instance, $\rho(r; i, L) = \langle \sigma(r; i, L) \rangle$ in disordered ferromagnets, and $\rho(r; i, L) = \langle \sigma(r; i, L) \rangle^2$ in spin glasses. For the random polymer models described in Sec. III, $\rho(r; i, L)$ corresponds to the contact density of monomer r [Eq. (44)]. Let

$\rho(i, L)$ denote the spatial average over all points r of the sample:

$$\rho(i, L) \equiv \frac{1}{L^d} \sum_{r \in L^d} \rho(r; i, L). \quad (1)$$

In a pure system, the exponent x_{pure} that governs the decay of the spatial average $\rho_{\text{pure}}(L)$ also describes the decay of the local parameter $\rho_{\text{pure}}(r; L)$ for any point r in the bulk:

$$\rho_{\text{pure}}(L) \sim \frac{1}{L^{x_{\text{pure}}}} \sim \rho_{\text{pure}}(r \in \text{bulk}; L). \quad (2)$$

In a disordered sample however, the spatial heterogeneity of the disorder induces a spatial heterogeneity in the local order parameter $\rho(r; i, L)$ at criticality. In particular, there exists a family of nontrivial exponents $x(q) \neq qx(1)$ [14] for the disorder-averaged powers of the local order parameter:

$$\overline{[\rho(r; i, L)]^q} \underset{L \rightarrow \infty}{\propto} \frac{1}{L^{x(q)}}. \quad (3)$$

In this formula, it is convenient to consider q as a continuous real parameter to probe also noninteger moments and even negative moments.

B. Introduction of a normalized multifractal measure

Since the multifractal formalism is usually defined for a normalized probability measure [1], it is convenient to construct a probability measure from the non-normalized observables one is interested in [10,11,28,29]. Here for the local order parameter, one defines in each sample (i) the spatial weights

$$w(r; i, L) = \frac{\rho(r; i, L)}{\sum_{r' \in L^d} \rho(r'; i, L)} = \frac{\rho(r; i, L)}{L^d \rho(i, L)} \quad (4)$$

normalized to

$$\sum_{r \in L^d} w(r; i, L) = 1. \quad (5)$$

So $w(r; i, L)$ represents the contribution of the site r to the order parameter of the sample i of size L^d . The statistics of these weights can be studied via the generalized moments

$$Y_q(i, L) = \sum_{r \in L^d} [w(r; i, L)]^q. \quad (6)$$

Deep in the ordered phase, where the order parameter $\rho(i, L)$ is finite as $L \rightarrow \infty$, the weights are expected to be of the same order $1/L^d$ [see Eq. (4)]. The decay of the generalized moments then follows the simple scaling

$$Y_q(i, L)|_{\text{ordered phase}} \sim \frac{1}{L^{(q-1)d}}. \quad (7)$$

At criticality, however, the generalized moments Y_q will display multifractality, with *a priori* different exponents for typical and averaged values.

C. Typical generalized dimensions $D(q)$

At criticality, the decay of typical values define a series of generalized exponents $\tau(q) = (q-1)D(q)$:

$$Y_q^{\text{typ}}(L) \equiv e^{\ln Y_q(i, L)} \sim \frac{1}{L^{\tau(q)}} = \frac{1}{L^{(q-1)D(q)}}. \quad (8)$$

The exponents $D(q)$ represent generalized dimensions [1]: $D(0)$ represents the dimension of the support of the measure; here, it is simply given by the space dimension

$$D(0) = d. \quad (9)$$

$D(1)$ is usually called the information dimension [1], since it describes the behavior of the ‘‘information’’ entropy

$$\begin{aligned} s(i, L) &\equiv - \sum_{r \in L^d} w(r; i, L) \ln w(r; i, L) = - \partial_q Y_q(i, L)|_{q=1} \\ &\simeq D(1) \ln L. \end{aligned} \quad (10)$$

Finally $D(2)$ is called the correlation dimension [1] and describes the decay of

$$Y_2^{\text{typ}}(L) \equiv e^{\ln Y_2(i, L)} \simeq L^{-D(2)}. \quad (11)$$

D. Typical singularity spectrum $f(\alpha)$

In the multifractal formalism, the singularity spectrum $f(\alpha)$ is given by the Legendre transform of $\tau(q)$ [1] via the standard formula

$$q = f'(\alpha), \quad (12)$$

$$\tau(q) = \alpha q - f(\alpha). \quad (13)$$

The physical meaning of $f(\alpha)$ is that the number $\mathcal{N}_L(\alpha)$ of points r where the weight $w(r; i, L)$ scales as $L^{-\alpha}$ typically behaves as

$$\mathcal{N}_L^{\text{typ}}(\alpha) \equiv e^{\ln \mathcal{N}_L(\alpha)} \propto L^{f(\alpha)}. \quad (14)$$

So the Legendre transform of Eq. (13) corresponds to the saddle-point calculus in α of the expression

$$Y_q^{\text{typ}}(L) \sim \int d\alpha L^{f(\alpha)} L^{-q\alpha}. \quad (15)$$

The general properties of the singularity spectrum $f(\alpha)$ are as follows [1]: it is positive $f(\alpha) \geq 0$ on an interval $[\alpha_{\min}, \alpha_{\max}]$ where $\alpha_{\min} = D(q = +\infty)$ is the minimal singularity exponent and $\alpha_{\max} = D(q = -\infty)$ is the maximal singularity exponent. It is concave $f''(\alpha) < 0$. It has a single maximum at some value α_0 where $f(\alpha_0) = D(q = 0)$, so here [Eq. (9)]

$$f(\alpha_0) = D(q = 0) = d. \quad (16)$$

The singularity exponent α_0 is thus the typical value

$$\alpha_0 = \alpha_{\text{typ}}. \quad (17)$$

However, the singularity that yields the leading contribution to the normalization $Y_1 = \sum_r w(r) = 1$ of the measure is the singularity exponent given by the information dimension $D(1)$ of Eq. (10):

$$\alpha_1 = f(\alpha_1) = D(1). \quad (18)$$

E. Generalized dimensions $\tilde{D}(q)$ defined from disorder-averaged values

Following [1], many authors consider that the singularity spectrum has a meaning only for $f(\alpha) \geq 0$ [10,11]. However, when multifractality arises in random systems, disorder-averaged values may involve other generalized exponents [30–33] than the typical values [see Eq. (8)]. In quantum localization transitions, these exponents were denoted by $\tilde{\tau}(q) = (q-1)\tilde{D}(q)$ in [12] and we will follow these notations:

$$\overline{Y_q(i,L)} \simeq \frac{1}{L^{\tilde{\tau}(q)}} = \frac{1}{L^{(q-1)\tilde{D}(q)}}. \quad (19)$$

For these disorder-averaged values, the corresponding singularity spectrum $\tilde{f}(\alpha)$ defined by

$$\overline{N_L(\alpha)} \propto L^{\tilde{f}(\alpha)} \quad (20)$$

may become negative $\tilde{f}(\alpha) < 0$ [12,30–33] to describe rare events.

F. Wiseman-Domany lack of self-averaging at criticality

To make the link between the exponents $x(q)$ defined from the powers of the local order parameter [Eq. (3)] and the multifractal exponents of the normalized weights [Eq. (4)] [28], one needs to use the equivalence between spatial average and disorder averages for the local order parameter.

1. Lack of self-averaging of extensive thermodynamic observables

In disordered systems off-criticality, the densities of extensive thermodynamic observables are self-averaging, because the finiteness of the correlation length $\xi(T)$ allows one to divide a large sample into independent large subsamples. At criticality however, this “subdivision” argument breaks down because of the divergence of $\xi(T_c) = \infty$ at T_c and a lack of self-averaging has been found at criticality whenever disorder is relevant [25–27]. More precisely, for a given observable X , it is convenient to define its normalized width as

$$R_X(T,L) \equiv \frac{\overline{X_i^2(T,L)} - [\overline{X_i(T,L)}]^2}{[\overline{X_i(T,L)}]^2}. \quad (21)$$

To be more specific, in ferromagnets, the observable X can be the magnetization M , the susceptibility χ , and the singular parts of the energy or of the specific heat [27]. In terms of the correlation length $\xi(T)$, the following behavior of $R_X(T,L)$ is expected [26,27].

(i) Off criticality, the correlation length $\xi(T)$ is finite. For $L \gg \xi(T)$, the system can be then divided into nearly independent subsamples and this leads to “strong self-averaging”

$$R_X(T,L) \sim \frac{1}{L^d} \text{ off criticality for } L \gg \xi(T). \quad (22)$$

(ii) In the critical region, when $L \ll \xi(T)$, the system cannot be divided anymore into nearly independent subsamples. In particular at T_c where $\xi(T_c) = \infty$, one can have either “weak self-averaging” for irrelevant disorder according to the Harris criterion [34], i.e., whenever the pure specific heat exponent $\alpha_{\text{pure}} = 2 - d\nu_{\text{pure}}$ is negative,

$$R_X(T_c(\infty), L) \sim L^{\alpha_{\text{pure}} \nu_{\text{pure}}} \text{ for irrelevant disorder } (\alpha_{\text{pure}} < 0), \quad (23)$$

or “no self-averaging,”

$$R_X(T_c(\infty), L) \sim Cst \text{ for random critical points.} \quad (24)$$

Note that for the marginal case $\alpha_{\text{pure}} = 0$ from the point of view of the Harris criterion, the power governing the weak self-averaging of Eq. (23) vanishes, so the ratio $R_X(T_c(\infty), L)$ can either remain finite as in Eq. (24) or vanish logarithmically.

2. Application to the powers of the local order parameter

Let us now apply these results to the spatial averages of powers of the local order parameter,

$$\rho_q(i,L) \equiv \frac{1}{L^d} \sum_{r \in L^d} [\rho(r;i,L)]^q, \quad (25)$$

which generalizes Eq. (1) to arbitrary q .

In the ordered phase, the strong self-averaging property of Eq. (22) means

$$\rho_q(i,L)|_{T < T_c} \simeq r_q(T) + \frac{v_q(i)}{L^{d/2}}, \quad (26)$$

where the leading term $r_q(T)$ is nonrandom and coincides with the disorder-averaged value in the thermodynamic limit $L \rightarrow \infty$,

$$r_q(T) = \lim_{L \rightarrow \infty} \{ \overline{[\rho(r;i,L)]^q} \}, \quad (27)$$

and where $v_q(i)$ is a random variable depending on the sample (i).

At criticality, the no self-averaging result of Eq. (24) means that the spatial averages defined in Eq. (25) behave asymptotically as

$$\rho_q(i,L) \simeq \frac{u_q(i)}{L^{x(q)}}, \quad (28)$$

where the exponent $x(q)$ is the exponent governing the decay of the disorder-averaged q moment $\overline{\rho^q(r;i,L)}$ of Eq. (3) and where $u_q(i)$ is a random variable of order $O(1)$ depending on sample (i).

In the following, we will use these result to understand the relations between the exponents for non-normalized observables and for the normalized measure. It will be useful to introduce the rescaled variable

$$u_q(i,L) \equiv L^{x(q)} \rho_q(i,L), \quad (29)$$

which remains a random variable $u_q(i)$ of order $O(1)$ in the limit $L \rightarrow \infty$.

G. Relation between the exponents $x(q)$ and $\tau(q)$

In terms of the local order parameter $\rho(r; i, L)$, the generalized moment $Y_q(i, L)$ reads from Eqs. (4) and (6)

$$Y_q(i, L) = \frac{\sum_{r \in L^d} \rho^q(r; i, L)}{\left(\sum_{r' \in L^d} \rho(r'; i, L) \right)^q}. \quad (30)$$

From Eq. (29) concerning the spatial averages of Eq. (25), one obtains

$$Y_q(i, L) = \frac{L^{d-x(q)} u_q(i, L)}{[L^{d-x(1)} u_1(i, L)]^q} = L^{d-x(q)-q[d-x(1)]} \frac{u_q(i, L)}{[u_1(i, L)]^q}. \quad (31)$$

The typical values of the random variables $u_q(i, L)$ in the limit $L \rightarrow \infty$ are of order $O(1)$ and thus the exponents $\tau(q)$ governing the typical values of Eq. (8) read

$$\tau(q) \equiv (q-1)D(q) = x(q) - d + q[d-x(1)], \quad (32)$$

or equivalently the typical generalized dimensions read

$$D(q) = d - \frac{qx(1) - x(q)}{q-1}. \quad (33)$$

So these relations given in Ref. [28] relate the exponents $x(q)$ of disorder-averaged moments of the local order parameter [Eq. (3)] to the typical exponents $\tau(q)$ of the normalized measure [Eq. (8)]. However, the exponents $\tilde{\tau}(q)$ of Eq. (19) cannot be simply related to $(x(q), \tau(q))$, since the disorder average of Eq. (31) may involve an L -dependent rare event contribution of the random variables $\frac{u_q(i, L)}{[u_1(i, L)]^q}$, in particular for large q , since q enters as a power in the denominator.

H. Conclusion for the statistics of the local order parameter

Let us now come back to our starting point: namely, the local order parameter $\rho(r; i, L)$ at site r . Using Eq. (29) for $q=1$, we obtain in terms of the weight of Eq. (4)

$$\rho(r; i, L) = w(r; i, L) [L^d \rho(i, L)] = w(r; i, L) L^{d-x(1)} u_1(i, L), \quad (34)$$

where $u_1(i, L)$ is a random variable of order $O(1)$. So the interpretation of the singularity spectrum $f(\alpha)$ for the weights given in Eq. (14) can be rephrased as follows: $\mathcal{N}_L(\alpha) \propto L^{f(\alpha)}$ represents the number of points r where the weight $w(r; i, L)$ scales as $L^{-\alpha}$ —i.e., the number of points r where the local order parameter scales as $\rho(r; i, L) \sim L^{-y}$ with

$$y = \alpha - d + x(1). \quad (35)$$

In particular, the typical exponent y_{typ} governing the logarithmic average

$$\overline{\ln \rho(r; i, L)} \underset{L \rightarrow \infty}{\propto} -y_{typ} \ln L \quad (36)$$

is related to the typical value α_{typ} of Eq. (17) by

$$y_{typ} = \alpha_{typ} - d + x(1). \quad (37)$$

Similarly, the minimal y_{min} and maximal y_{max} exponents are related to $\alpha_{min} = D(q = +\infty)$ and $\alpha_{max} = D(q = -\infty)$. In particular, since the minimum value y_{min} cannot be negative, one has the bound

$$y_{min} = \alpha_{min} - d + x(1) \geq 0. \quad (38)$$

I. Critical region

Both in quantum localization [10–12] and in disordered ferromagnets [14], the multifractal statistics exactly at T_c is expected to coexist with a single correlation length exponent ν outside T_c . More precisely, the powers of the local order parameters are expected to follow the finite-size scaling form in the critical region around T_c [Eq. (3)]:

$$\overline{[\rho(r; i, L; T)]^q} \underset{L \rightarrow \infty}{\propto} \frac{1}{L^{x(q)}} \Phi_q((T - T_c) L^{1/\nu}). \quad (39)$$

For $T < T_c$, the convergence to finite values $\overline{[\rho(r; L = \infty; T)]^q}$ in the $L \rightarrow \infty$ limit yields

$$\overline{[\rho(r; L = \infty; T)]^q} = (T_c - T)^{\beta(q)} \quad \text{with } \beta(q) = \nu x(q). \quad (40)$$

So the presence of a multifractal spectrum $x(q) \neq qx(1)$ at criticality corresponds to nontrivial exponents $\beta(q) \neq q\beta(1)$ for the powers of the local order parameters in the ordered phase.

III. WETTING AND POLAND-SCHERAGA TRANSITIONS

A. Wetting and Poland-Scheraga models

Wetting transitions are in some sense the simplest phase transitions, since they involve linear systems [35,36]. Let us consider a one-dimensional random walk (RW) of $2L$ steps, starting at $z(0)=0$, with increments $z(r+1)-z(r)=\pm 1$. The random walk is constrained to remain in the upper half plane $z \geq 0$, but gains an adsorption energy ϵ_r if $z(r)=0$. More precisely, the model is defined by the partition function

$$Z_{wetting}(2L) = \sum_{RW} \exp\left(\beta \sum_{1 \leq r \leq L} \epsilon_r \delta_{z_r, 0}\right), \quad (41)$$

with inverse temperature $\beta=1/T$. In the pure case $\epsilon_r = \epsilon_0$, there exists a continuous phase transition between a localized phase at low temperature, characterized by an extensive number of contacts at $z=0$, and a delocalized phase at high temperature.

The Poland-Scheraga (PS) model of DNA denaturation [37] is closely related to the wetting model. It describes the configuration of the two complementary chains as a sequence of bound segments and open loops. Each loop of length l has a polymeric entropic weight $\mathcal{N}(l) \sim \mu^l/l^c$, whereas each contact at position r has a Boltzmann weight $e^{-\beta \epsilon_r}$. We assume that the two chains are bound at $r=1$ and $r=L$. The partial partition function $Z_{PS}(r)$ with bound ends then satisfies the simple recursion relation

$$Z_{PS}(r) = e^{-\beta\epsilon_r} \sum_{r'=1}^{r-1} \mathcal{N}(r-r') Z_{PS}(r'). \quad (42)$$

The wetting model (41) corresponds to a Poland-Scheraga model with loop exponent $c=3/2$ (this exponent comes from the first return distribution of a one-dimensional random walk). For DNA denaturation, the appropriate value of the loop exponent c has been the source of some debate. Gaussian loops in $d=3$ dimensions are characterized by $c=d/2=3/2$. The role of self-avoidance within a loop was taken into account by Fisher [38] and yields the larger value $c=d\nu_{SAW}\sim 1.76$, where ν_{SAW} is the surface-acoustic-wave (SAW) radius of gyration exponent in $d=3$. More recently, Monte Carlo simulations of self-avoiding walks [39,40] and theoretical arguments [41] pointed towards a value $c>2$.

B. Disorder relevance as a function of the loop exponent c

The Harris criterion concerning the stability of pure second-order transitions with respect to disorder relies on the sign of the specific heat exponent

$$\alpha_p = 2 - \nu_p = \frac{2c-3}{c-1}. \quad (43)$$

Disorder is thus irrelevant for $1 < c < \frac{3}{2}$, marginal for $c = \frac{3}{2}$, and relevant for $\frac{3}{2} < c < 2$. Poland-Scheraga models are thus particularly interesting to study disorder effects on pure phase transitions, since the parameter c allows one to study, within a single model, the various cases of second-order transitions with, respectively, marginal or relevant disorder according to the Harris criterion or first-order transition. From this point of view, it is reminiscent of the two-dimensional (2D) Potts model, where the pure critical properties vary with the parameter q : the transition is second order for $q < 4$, the Ising case $q=2$ corresponding to the marginal case of the Harris criterion, whereas the transition becomes first order for $q > 4$. The marginal case $c = \frac{3}{2}$ has been studied for a long time [42–49] and is of special interest since it corresponds to two-dimensional wetting as explained above.

C. Numerical details

In the following, we will study the multifractal properties of the local contact density

$$\rho(r; i, L) \equiv \langle \delta_{z_r, 0} \rangle_{i, L} \quad (44)$$

representing the probability that the monomer r of the sample (i) of length L is on the interface $z=0$ at criticality $T=T_c$. We have chosen the same disorder distribution and parameters as in our previous work [49], and we have used the same Fixman-Freire scheme to speed up calculations, as explained in detail in [48,49]. The results presented below have been obtained for the following sizes L and the corresponding number $n_s(L)$ of disordered samples:

$$\frac{L}{10^3} = 16, 32, 64, 128, 256, 512, \quad (45)$$

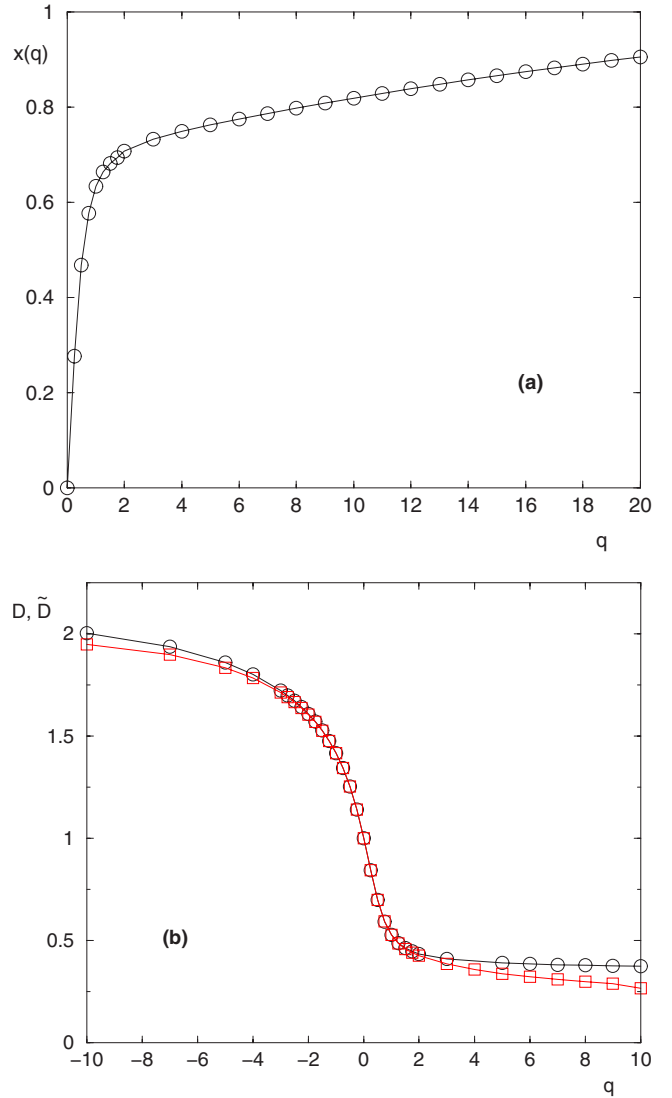


FIG. 1. (Color online) Wetting with loop exponent $c=1.75$. (a) Exponents $x(q)$ governing the decay of the disorder averaged q th powers of the local order parameter [Eq. (47)]. (b) Generalized dimensions $D(q)$ (\circ) and $\tilde{D}(q)$ (\square) associated, respectively, with the typical values [Eq. (8)] and to disorder-averaged values [Eq. (19)] of the generalized moments [Eq. (51)].

$$\frac{n_s(L)}{10^4} = 500, 250, 120, 60, 30, 15. \quad (46)$$

IV. MULTIFRACTAL ANALYSIS OF THE WETTING TRANSITION WITH LOOP EXPONENT $c=1.75$

In this section, we describe our results for the wetting transition with loop exponent $c=1.75$, which corresponds to relevant disorder as explained above [Eq. (43)].

A. Exponents $x(q)$ and generalized dimensions $D(q)$ and $\tilde{D}(q)$

We show in Fig. 1(a) the scaling dimensions $x(q)$ governing the disorder-averaged moments of the local contact density [Eq. (3)]:

$$\overline{\langle \delta_{z,r,0} \rangle^q} \propto \frac{1}{L^{x(q)}}. \quad (47)$$

It is strongly nonlinear $x(q) \neq qx(1)$. Some particular values are

$$x(q=1) \simeq 0.63, \quad (48)$$

$$x(q=2) \simeq 0.71. \quad (49)$$

In the large- q limit, it saturates towards

$$x(q \rightarrow +\infty) \rightarrow 1. \quad (50)$$

This point will be discussed in detail in Sec. VI.

In Fig. 1(b), we show the generalized dimensions $D(q)$ and $\tilde{D}(q)$ associated, respectively, with the typical values [Eq. (8)] and with disorder-averaged values [Eq. (19)] of the generalized moments [Eq. (6)]:

$$Y_q(i,L) = \frac{\sum_r \langle \delta_{z,r,0} \rangle^q}{\left(\sum_{r'} \langle \delta_{z,r',0} \rangle \right)^q}. \quad (51)$$

In particular, the information dimension of Eq. (10) is

$$D(q=1) = \tilde{D}(1) \simeq 0.59 \quad (52)$$

and the correlation dimension of Eq. (11) is

$$D(q=2) \sim \tilde{D}(2) \simeq 0.44. \quad (53)$$

For q large enough, the two exponents do not coincide anymore, $D(q) \neq \tilde{D}(q)$, as expected from the discussion of Eqs. (31)–(33).

B. Typical singularity spectrum $f(\alpha)$

To measure the typical singularity spectrum introduced in Eq. (14), we have used the standard method based on q measures of Ref. [50]. We show in Fig. 2(a) the curve $f(\alpha)$. The maximum corresponds to the typical exponent α_0 [Eq. (17)]:

$$\alpha_{typ} = \alpha_0 = 1.53. \quad (54)$$

The curve is tangent to the diagonal $\alpha=f(\alpha)$ at the point [Eq. (18)]

$$\alpha_1 = f(\alpha_1) = D(1) \simeq 0.59. \quad (55)$$

The minimal value corresponds to

$$\alpha_{min} = D(q \rightarrow +\infty) \simeq 0.36 \quad (56)$$

and the maximal value

$$\alpha_{max} = D(q \rightarrow -\infty) \simeq 2.22. \quad (57)$$

In Fig. 2(b), we show the corresponding curve $\alpha(q)$ representing the dominant exponent α that contributes to the q -generalized moment [Eq. (15)].

C. Disorder-averaged singularity spectrum $\tilde{f}(\alpha)$

In contrast to the method of [50], which allows one to measure numerically the typical spectrum, we are not aware

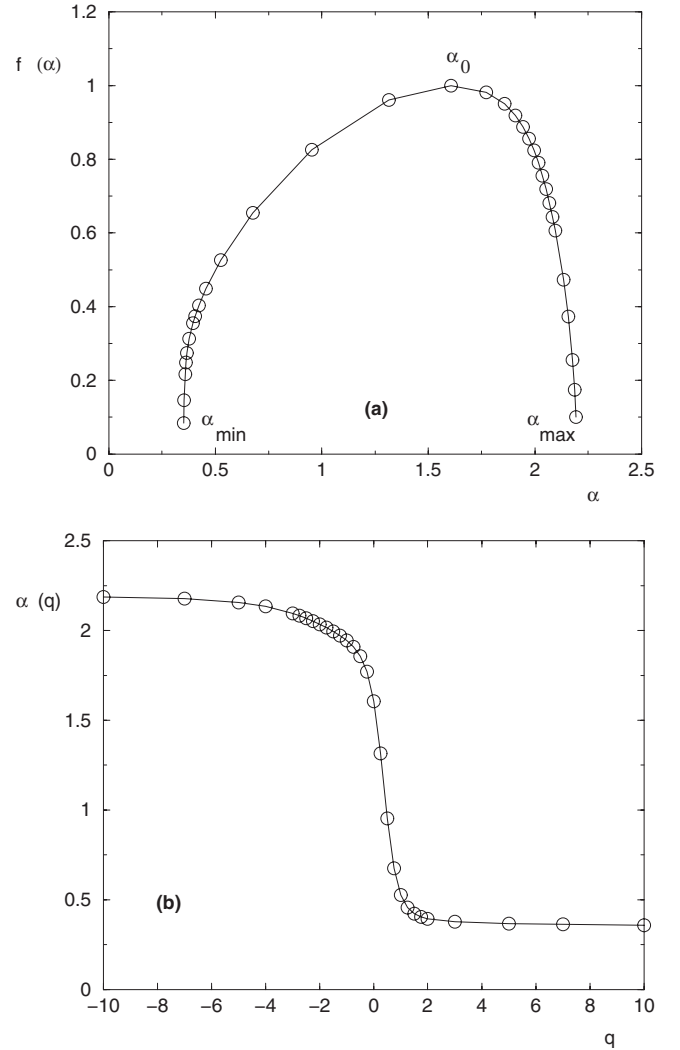


FIG. 2. Wetting with loop exponent $c=1.75$. (a) Typical singularity spectrum $f(\alpha)$ [Eq. (14)]: the maximum occurs at $\alpha_0 \sim 1.53$ which represents the typical value. The minimal value is around $\alpha_{min} \simeq 0.36$. (b) Corresponding curve $\alpha(q)$.

of an efficient method to measure the disorder-averaged singularity spectrum $\tilde{f}(\alpha)$. We have thus measured the probability distributions $H_L(\alpha)$ of the rescaled weights

$$\alpha = - \frac{\ln w(r;i,L)}{\ln L} \quad (58)$$

in analogy with similar numerical measures of the multifractal spectrum from the statistics of correlation function in disordered Potts models [16,17]. Our results presented in Fig. 3 show that the convergence towards the typical spectrum $f(\alpha)$ in the positive region $\alpha > 0$ is extremely slow. In particular, the convergence of the most probable exponent $\alpha_{mp}(L)$ towards the typical value α_0 is extremely slow, of the order of $1/\ln(L)$.

D. Histograms of the information entropy and of Y_2

We show in Fig. 4(a) the histogram over the samples (i) of the information entropy $s(i,L)$ defined in Eq. (10): as L

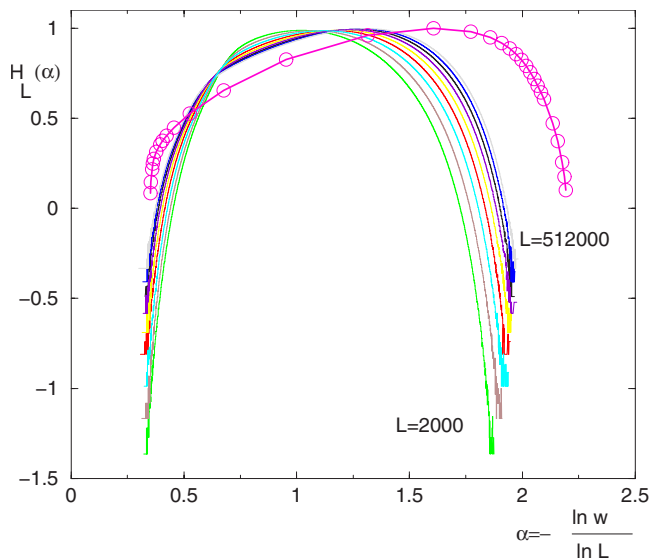


FIG. 3. (Color online) Wetting with loop exponent $c=1.75$: the histograms $H_L(\alpha)$ of the rescaled variable $\alpha = -\frac{\ln w(r; i, L)}{\ln L}$ shown for $2 \times 10^3 \leq L \leq 512 \times 10^3$ converge extremely slowly [as $1/\ln(L)$] towards the typical singularity spectrum $f(\alpha)$ (\circ) measured with the method of Ref. [50].

grows, the averaged value grows logarithmically [Eq. (10)],

$$\overline{s(i, L)} \approx D(1) \ln L, \quad (59)$$

whereas the width converges towards a constant value.

Similarly, we show in Fig. 4(b) the histogram over the samples (i) of $\ln Y_2(i, L)$ [Eq. (6)]: as L grows, the averaged value grows logarithmically [Eq. (11)],

$$\overline{\ln Y_2(i, L)} \approx -D(2) \ln L, \quad (60)$$

whereas the width converges towards a constant value.

E. Statistics of the spatially averaged order parameter over the samples

To study the Wiseman-Domany lack of self-averaging at criticality for the spatial average $\rho(i, L)$ of the order parameter [Eq. (28)], we have computed the probability distribution $G_L(u)$ of the ratio

$$u = \frac{\rho(i, L)}{\overline{\rho(i, L)}}. \quad (61)$$

The results for various L presented in Fig. 5 show that u remains a random variable of order $O(1)$ in the limit $L \rightarrow \infty$.

V. MULTIFRACTAL ANALYSIS OF THE WETTING TRANSITION WITH LOOP EXPONENT $c=1.5$

In this section, we describe our results for the wetting transition with loop exponent $c=1.5$, which corresponds to marginal disorder as explained above [Eq. (43)].

A. Exponents $x(q)$ and generalized dimensions $D(q)$ and $\tilde{D}(q)$

We show in Fig. 6(a) the scaling dimensions $x(q)$ governing the disorder-averaged moments of the local contact density [Eq. (3)]:

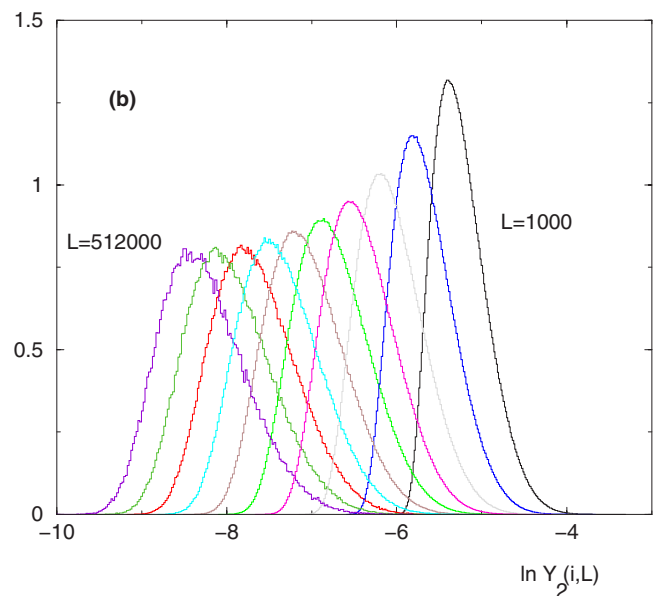
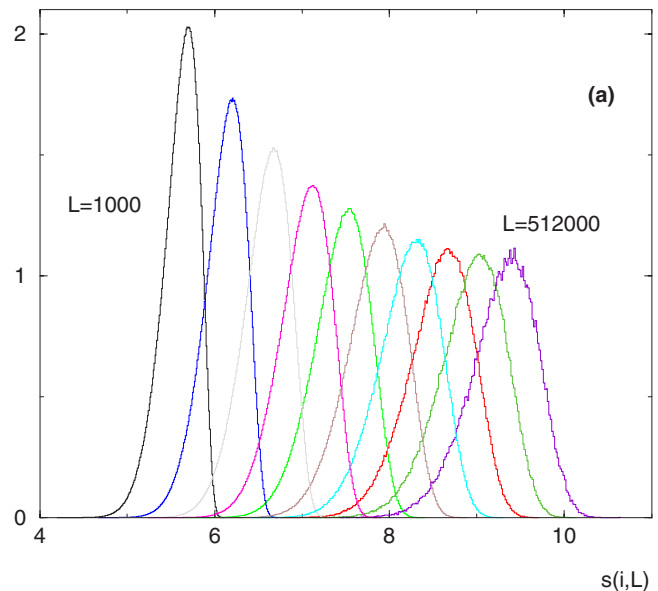


FIG. 4. (Color online) Wetting with loop exponent $c=1.75$. (a) Histogram over the samples of the information entropy $s(i, L)$ defined in Eq. (10) for sizes $10^3 \leq L \leq 512 \times 10^3$: the averaged value grows as $\overline{s(i, L)} \approx D(1) \ln L$. (b) Histogram over the samples of $\ln Y_2(i, L)$ [Eq. (6)] for sizes $10^3 \leq L \leq 512 \times 10^3$: the averaged value behaves as $\overline{\ln Y_2(i, L)} \approx -D(2) \ln L$.

$$\overline{\langle \delta_{z,r,0} \rangle^q} \propto \frac{1}{L^{x(q)}}. \quad (62)$$

It is strongly nonlinear, $x(q) \neq qx(1)$. Some particular values are

$$x(q=1) \approx 0.52, \quad (63)$$

$$x(q=2) \approx 0.79. \quad (64)$$

In the large- q limit, it saturates towards

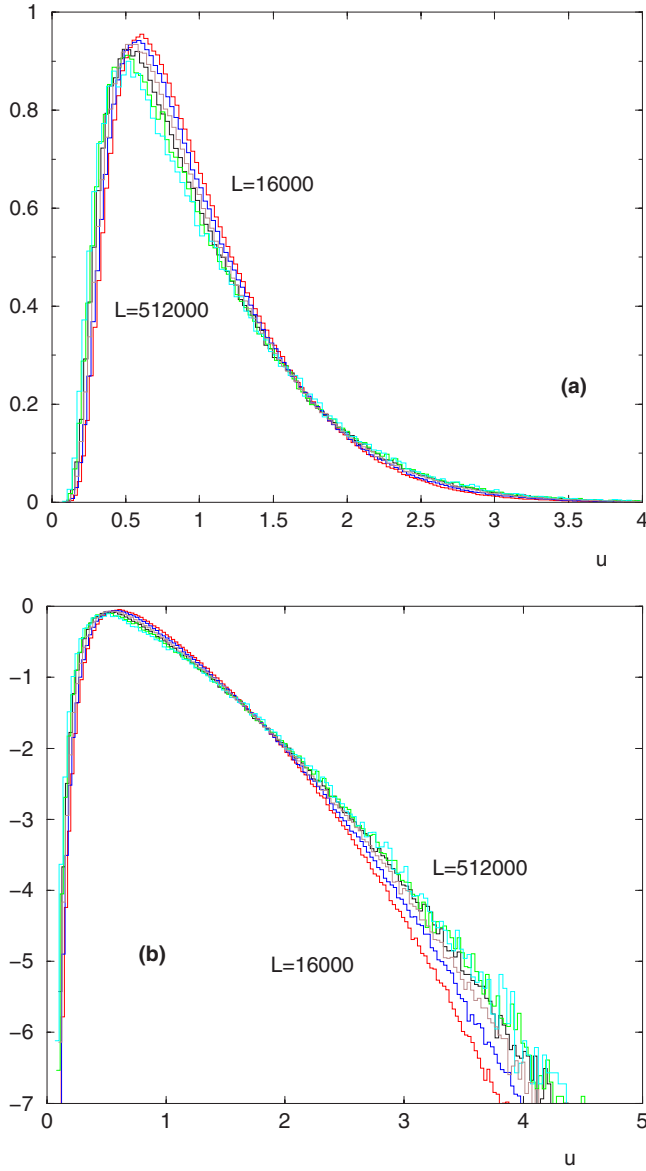


FIG. 5. (Color online) Wetting with loop exponent $c=1.75$: Wiseman-Domany lack of self-averaging at criticality for the spatial average $\rho(i,L)$ of the order parameter [Eq. (1)]. (a) Histogram over the samples of the variable $u=\rho(i,L)/\rho(i,L)$ for sizes $16 \times 10^3 \leq L \leq 512 \times 10^3$: u remains a random variable of order $O(1)$ in the limit $L \rightarrow \infty$. (b) Same data in logarithmic scale.

$$x(q \rightarrow +\infty) \rightarrow 1 \quad (65)$$

(see the discussion of Sec. VI).

In Fig. 6(b) we show the generalized dimensions $D(q)$ and $\tilde{D}(q)$ associated, respectively, with the typical values [Eq. (8)] and with disorder-averaged values [Eq. (19)] of the generalized moments [Eq. (6)]:

$$Y_q(i,L) = \frac{\sum_r \langle \delta_{z_r,0} \rangle^q}{\left(\sum_{r'} \langle \delta_{z_{r'},0} \rangle \right)^q}. \quad (66)$$

In particular, the information dimension of Eq. (10) is

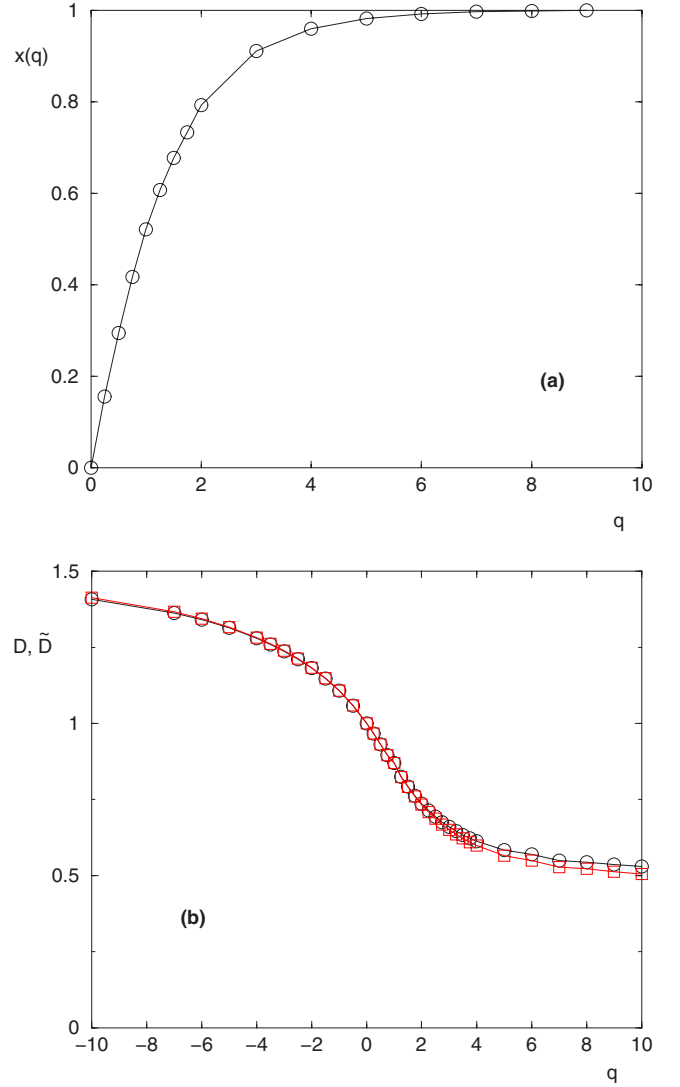


FIG. 6. (Color online) Wetting with loop exponent $c=1.5$. (a) Exponents $x(q)$ governing the decay of the disorder-averaged q th powers of the local order parameter [Eq. (62)]. (b) Generalized dimensions $D(q)$ (\circ) and $\tilde{D}(q)$ (\square) associated, respectively, with the typical values [Eq. (8)] and with disorder-averaged values [Eq. (19)] of the generalized moments [Eq. (66)].

$$D(q=1) = \tilde{D}(1) \approx 0.87 \quad (67)$$

and the correlation dimension of Eq. (11) is

$$D(q=2) \sim \tilde{D}(2) \approx 0.74. \quad (68)$$

B. Typical singularity spectrum $f(\alpha)$

We show in Fig. 7(a) the curve $f(\alpha)$ obtained via the standard method of Ref. [50]. The maximum corresponds to the typical exponent α_0 [Eq. (17)]

$$\alpha_{typ} = \alpha_0 = 1.125. \quad (69)$$

The curve is tangent to the diagonal $\alpha=f(\alpha)$ at the point [Eq. (18)]

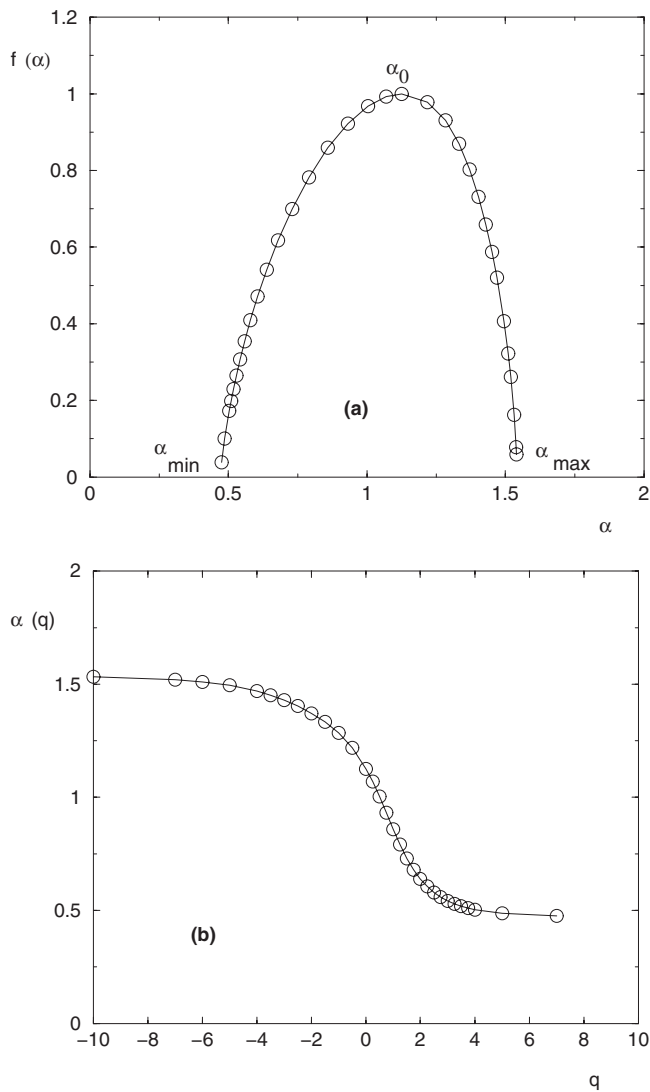


FIG. 7. Wetting with loop exponent $c=1.5$. (a) Typical singularity spectrum $f(\alpha)$ [Eq. (14)]: the maximum occurs at $\alpha_0 \sim 1.125$ which represents the typical value. The minimal value is around $\alpha_{min} \approx 0.48$. (b) Corresponding curve $\alpha(q)$.

$$\alpha_1 = f(\alpha_1) = D(1) \approx 0.87. \quad (70)$$

The minimal value corresponds to

$$\alpha_{min} = D(q = +\infty) \approx 0.48 \quad (71)$$

and the maximal value

$$\alpha_{max} = D(q = -\infty) \approx 1.53. \quad (72)$$

In Fig. 7(b), we show the corresponding curve $\alpha(q)$ representing the dominant exponent α that contributes to the q -generalized moment [Eq. (15)].

C. Disorder-averaged singularity spectrum $\tilde{f}(\alpha)$

We show in Fig. 8 the histograms $H_L(\alpha)$ of

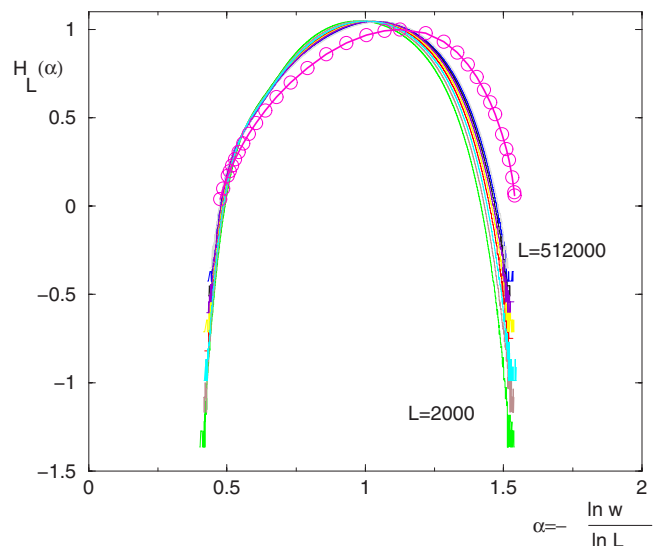


FIG. 8. (Color online) Wetting with loop exponent $c=1.5$: the histograms $H_L(\alpha)$ of the rescaled variable $\alpha = -\frac{\ln w(r; i, L)}{\ln L}$ shown for $2 \times 10^3 \leq L \leq 512 \times 10^3$ converge extremely slowly [as $1/\ln(L)$] towards the typical singularity spectrum $f(\alpha)$ (○) measured with the method of Ref. [50].

$$\alpha = -\frac{\ln w(r; i, L)}{\ln L} \quad (73)$$

for various sizes L and compare with the typical spectrum $f(\alpha)$ obtained via the method of Ref. [50]. As previously mentioned for the corresponding Fig. 3 concerning the case $c=1.75$, the convergence is extremely slow, of the order of $1/\ln(L)$.

D. Histograms of the information entropy and of Y_2

We show in Fig. 9(a) the histogram over the samples (i) of the information entropy $s(i, L)$ defined in Eq. (10): as L grows, the averaged value grows logarithmically [Eq. (10)],

$$\overline{s(i, L)} \approx D(1) \ln L, \quad (74)$$

whereas the width again converges towards a constant value.

Similarly, we show in Fig. 9(b) the histogram over the samples (i) of $\ln Y_2(i, L)$ [Eq. (6)]: as L grows, the averaged value grows logarithmically [Eq. (11)],

$$\overline{\ln Y_2(i, L)} \approx -D(2) \ln L, \quad (75)$$

whereas (q) the width converges towards a constant value.

E. Statistics of the spatial-averaged order parameter over the samples

To study the Wiseman-Domany lack of self-averaging at criticality for the spatial average $\rho(i, L)$ of order parameter [Eq. (28)], we have computed the probability distribution $G_L(u)$ of the ratio

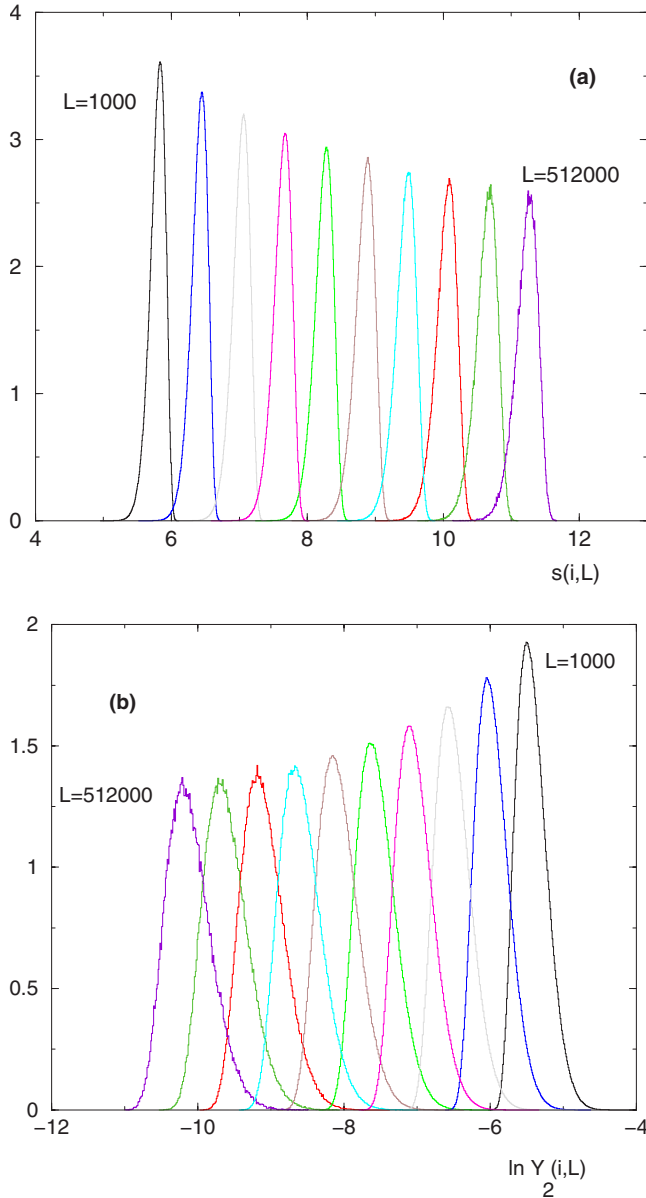


FIG. 9. (Color online) Wetting with loop exponent $c=1.5$. (a) Histogram over the samples of the information entropy $s(i,L)$ defined in Eq. (10) for sizes $10^3 \leq L \leq 512 \times 10^3$: the averaged value grows as $s(i,L) \approx D(1) \ln L$. (b) Histogram over the samples of $\ln Y_2(i,L)$ [Eq. (6)] for sizes $10^3 \leq L \leq 512 \times 10^3$: the averaged value behaves as $\ln Y_2(i,L) \approx -D(2) \ln L$.

$$u = \frac{\rho(i,L)}{\rho(i,L)}. \quad (76)$$

The results for various L are shown in Fig. 10 and show that u remains a random variable of order $O(1)$ in the limit $L \rightarrow \infty$.

VI. INFLUENCE OF BOUNDARY CONDITIONS

A. Value $x(q \rightarrow \infty)$ and minimal value α_{min} of the multifractal spectrum

In our numerical studies for $c=1.75$ and $c=1.5$ presented above, we have found in both cases that the exponents $x(q)$

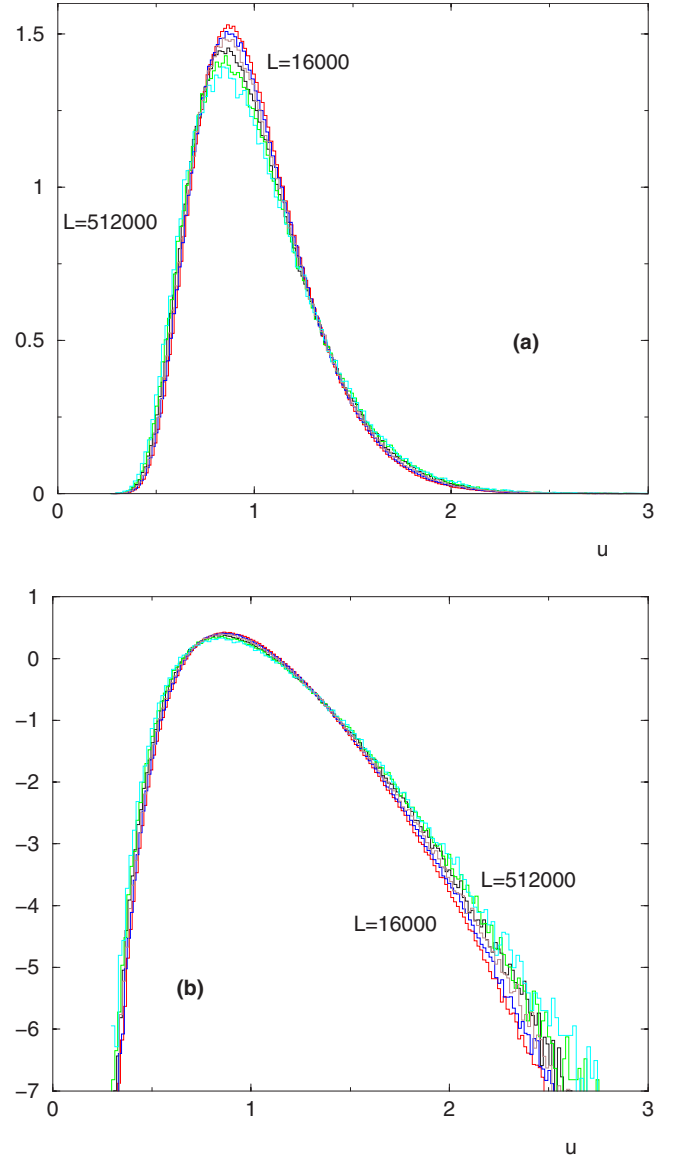


FIG. 10. (Color online) Wetting with loop exponent $c=1.5$: Wiseman-Domany lack of self-averaging at criticality for the spatial average $\rho(i,L)$ of the order parameter [Eq. (1)]. (a) Histogram over the samples of the variable $u = \rho(i,L)/\rho(i,L)$ for sizes $16 \times 10^3 \leq L \leq 512 \times 10^3$: u remains a random variable of order $O(1)$ in the limit $L \rightarrow \infty$. (b) Same data in logarithmic scale.

governing the decay of the powers of the local order parameter [Eq. (3)] saturate to 1 for large q [Eqs. (50) and (62)]:

$$x(q \rightarrow \infty) = 1. \quad (77)$$

This indicates that moments of high order $q \rightarrow \infty$ are dominated by a finite number of points (of density of order $1/L$) having a finite order parameter $O(1)$. So the minimal y_{min} actually saturates the bound of Eq. (38):

$$y_{min} = \alpha_{min} - d + x(1) = 0. \quad (78)$$

As a consequence, the minimal value α_{min} of the multifractal spectrum is simply given by

$$\alpha_{min} = d - x(1). \quad (79)$$

This simple relation is satisfied by the above numerical results for both $c=1.75$ [with $x(q=1) \simeq 0.63$ and $\alpha_{min} = D(q=+\infty) \simeq 0.36$] and for $c=1.5$ [with $x(q=1) \simeq 0.52$ and $\alpha_{min} = D(q=+\infty) \simeq 0.48$].

To determine whether these properties are linked to the bound-bound boundary conditions used or are more general, we have studied other boundary conditions as we now explain.

B. Comparison between fixed and free boundary conditions

In the previous Secs. IV and V, we have presented numerical results concerning the bound-bound boundary conditions, where the polymer is attached to the interface $z=0$ at both ends:

$$z(r=1) = 0 = z(r=L). \quad (80)$$

Since the wetting models cannot be directly defined with completely free boundary conditions (since the space above the interface is infinite), we have still considered the bound-bound boundary conditions of Eq. (80) but we have measured the multifractal spectrum using only the ‘‘bulk monomers’’ satisfying

$$\frac{L}{4} \leq r \leq \frac{3L}{4}. \quad (81)$$

This procedure aims to simulate ‘‘free’’ boundary conditions at $r=\frac{L}{4}$ and $r=\frac{3L}{4}$ for a sample of size $\frac{L}{2}$. The singularity spectra measured with these two types of boundary conditions are shown in Figs. 11(a) and 11(b) for the cases $c=1.75$ and $c=1.5$, respectively. These singularity spectra coincide within our numerical accuracy [the difference in the right half of Fig. 11(a) corresponds to the negative moments $q < 0$ dominated by the smallest weights whose statistics is more difficult to measure precisely].

C. Griffiths-ordered clusters

In particular, the fact that the minimal value α_{min} remains the same for fixed and free boundary conditions shows that the finite number of points having a finite order parameter are not confined to the boundaries but also exist in the bulk at criticality. This is related to the finite probability of finite ordered clusters in diluted disordered systems below the pure critical temperature, which have been much studied in the context of Griffiths singularities [51].

Our conclusion for the wetting transition and more generally for disordered systems at criticality is that the finite probability of Griffiths-ordered clusters determines the asymptotic value

$$x(q \rightarrow \infty) = d \quad (82)$$

of the exponents $x(q)$ governing the decay of the powers of the local order parameter. Accordingly, the minimal y_{min} saturates the bound of Eq. (38),

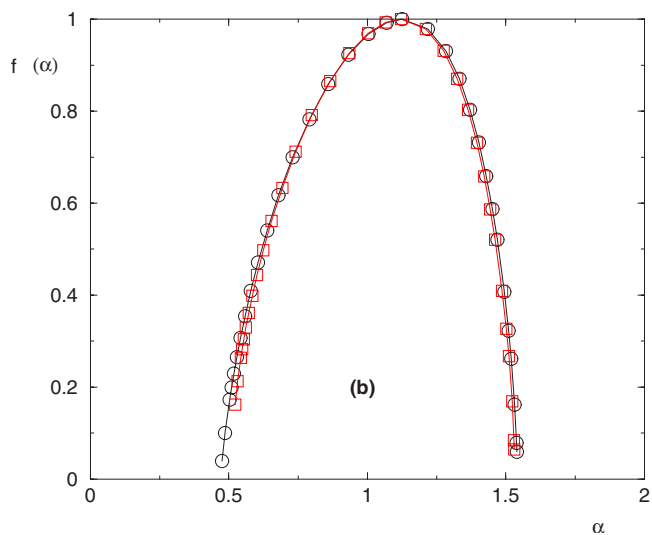
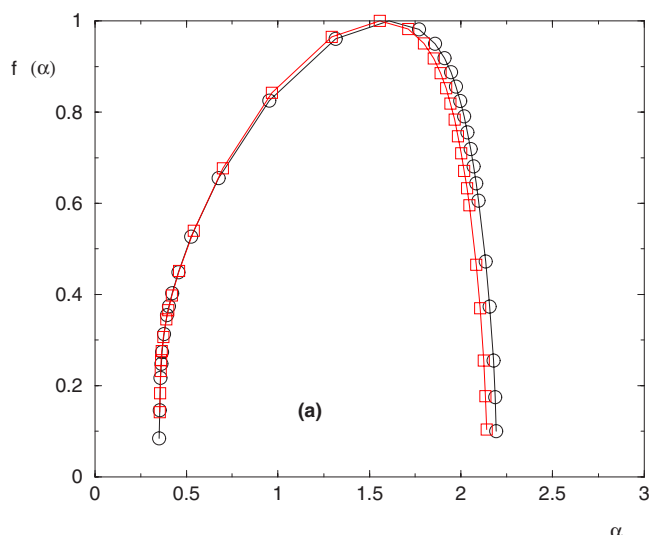


FIG. 11. (Color online) Typical singularity spectra $f(\alpha)$ for bound-bound (○) or free-free (□) boundary conditions. (a) Wetting with loop exponent $c=1.75$. (b) Wetting with loop exponent $c=1.5$.

$$y_{min} = \alpha_{min} - d + x(1) = 0, \quad (83)$$

and the minimal value α_{min} of the multifractal spectrum is simply related to the exponent $x(1)$ governing the decay of the order parameter:

$$\alpha_{min} = d - x(1). \quad (84)$$

VII. SUMMARY AND CONCLUSIONS

In this paper, we have studied in detail the multifractal statistics of the local order parameter at random wetting critical points for two values of the loop exponents c : namely, $c=1.75$ and $c=1.5$. For these models where large sizes up to $L=512 \times 10^3$ can be probed with a good statistics over the samples, we have numerically measured (i) the ‘‘Ludwig exponents’’ $x(q)$ that govern the moments $\rho^q(r)$ of the local order parameter $\rho(r)$, (ii) the generalized dimensions $D(q)$

and $\tilde{D}(q)$ associated with typical and disorder-averaged values of the moments $Y_q = \sum_r w^q(r)$ of the multifractal measure $w(r) = \rho(r) / [\sum_{r'} \rho(r')]$, and (iii) the corresponding typical singularity spectrum $f(\alpha)$.

We have also discussed the relations between this multifractal statistics and the Wiseman-Domany lack of self-averaging at criticality. Finally, we have argued that the presence of finite Griffiths-ordered clusters at T_c determines the asymptotic value of the Ludwig exponent $x(q \rightarrow \infty) = d$ and the minimal value $\alpha_{min} = D(q \rightarrow \infty) = d - x(1)$ of the multifractal spectrum. We have checked that these relations are well satisfied in our numerical results for the wetting transitions

(where $d=1$), not only for bound-bound boundary conditions, but also for free-free boundary conditions.

However, finite Griffiths-ordered clusters occur above critical points in disordered systems independently of the relevance or irrelevance of the disorder from the Harris criterion [51], which concerns coarse-grained properties at weak disorder. Our conclusion is thus that the multifractal statistics of the local order parameter should be nontrivial for any critical point with frozen disorder, since it probes the heterogeneities at all scales. This would explain why our results concerning the marginal disorder case $c=1.5$ are qualitatively similar to our results for the relevant disorder case $c=1.75$.

-
- [1] T. C. Halsey, M. H. Jensen, L. P. Kadanoff, I. Procaccia, and B. I. Shraiman, *Phys. Rev. A* **33**, 1141 (1986).
- [2] G. Paladin and A. Vulpiani, *Phys. Rep.* **156**, 147 (1987).
- [3] H. E. Stanley and P. Meakin, *Nature (London)* **335**, 405 (1988).
- [4] *Fractals in Physics, essays in honour of B.B. Mandelbrot*, edited by A. Aharony and J. Feder (North Holland, Amsterdam, 1990).
- [5] P. Meakin, *Fractals, Scaling and Growth far from Equilibrium* (Cambridge University Press, Cambridge, England, 1998).
- [6] D. Harte, *Multifractals, Theory and Applications* (Chapman and Hall, London, 2001).
- [7] B. Duplantier, in *Mathematical Statistical Physics*, Proceedings of the Les Houches Summer School of Theoretical Physics, Les Houches, 2005, edited by A. Bovier *et al.* (Elsevier, Amsterdam, 2006), Session LXXXIII, p. 101.
- [8] F. Wegner, *Z. Phys. B* **36**, 209 (1980).
- [9] C. Castellani and L. Peliti, *J. Phys. A* **19**, L429 (1986).
- [10] M. Janssen, *Int. J. Mod. Phys. B* **8**, 943 (1994); *Phys. Rep.* **295**, 1 (1998).
- [11] B. Huckestein, *Rev. Mod. Phys.* **67**, 357 (1995).
- [12] F. Evers and A. D. Mirlin, *Phys. Rev. Lett.* **84**, 3690 (2000); A. D. Mirlin and F. Evers, *Phys. Rev. B* **62**, 7920 (2000); F. Evers, A. Mildenerger, and A. D. Mirlin, *ibid.* **64**, 241303R (2001); A. Mildenerger, F. Evers, and A. D. Mirlin, *ibid.* **66**, 033109 (2002); A. D. Mirlin, Y. V. Fyodorov, A. Mildenerger, and F. Evers, *Phys. Rev. Lett.* **97**, 046803 (2006).
- [13] C. Monthus and T. Garel, *Phys. Rev. E* **75**, 051122 (2007).
- [14] A. W. W. Ludwig, *Nucl. Phys. B* **330**, 639 (1990).
- [15] J. L. Jacobsen and J. L. Cardy, *Nucl. Phys. B* **515**, 701 (1998).
- [16] T. Olson and A. P. Young, *Phys. Rev. B* **60**, 3428 (1999).
- [17] C. Chatelain and B. Berche, *Nucl. Phys. B* **572**, 626 (2000).
- [18] G. Palágyi, C. Chatelain, B. Berche, and F. Iglói, *Eur. Phys. J. B* **13**, 357 (2000).
- [19] N. Sourlas, *Europhys. Lett.* **3**, 1007 (1987).
- [20] M. J. Thill and H. J. Hilhorst, *J. Phys. I* **6**, 67 (1996).
- [21] G. Parisi and N. Sourlas, *Phys. Rev. Lett.* **89**, 257204 (2002).
- [22] E. Nogueira, Jr., S. Coutinho, F. D. Nobre, E. M. F. Curado, and J. R. L. de Almeida, *Phys. Rev. E* **55**, 3934 (1997).
- [23] J. Kisker and A. P. Young, *Phys. Rev. B* **58**, 14397 (1998); F. Iglói, R. Juhasz, and H. Rieger, *ibid.* **61**, 11552 (2000).
- [24] F. Iglói and C. Monthus, *Phys. Rep.* **412**, 277 (2005).
- [25] S. Wiseman and E. Domany, *Phys. Rev. E* **52**, 3469 (1995).
- [26] A. Aharony and A. B. Harris, *Phys. Rev. Lett.* **77**, 3700 (1996).
- [27] S. Wiseman and E. Domany, *Phys. Rev. Lett.* **81**, 22 (1998); *Phys. Rev. E* **58**, 2938 (1998).
- [28] B. Duplantier and A. W. W. Ludwig, *Phys. Rev. Lett.* **66**, 247 (1991).
- [29] W. Pook and M. Janssen, *Z. Phys. B: Condens. Matter* **82**, 295 (1991).
- [30] B. Mandelbrot, *Physica A* **163**, 306 (1990); *J. Stat. Phys.* **110**, 739 (2003).
- [31] A. B. Chhabra and K. R. Sreenivasan, *Phys. Rev. A* **43**, 1114 (1991).
- [32] M. H. Jensen, G. Paladin, and A. Vulpiani, *Phys. Rev. E* **50**, 4352 (1994).
- [33] T. C. Halsey, K. Honda, and B. Duplantier, *J. Stat. Phys.* **85**, 681 (1996); T. C. Halsey, B. Duplantier, and K. Honda, *Phys. Rev. Lett.* **78**, 1719 (1997).
- [34] A. B. Harris, *J. Phys. C* **7**, 1671 (1974).
- [35] M. E. Fisher, *J. Stat. Phys.* **34**, 667 (1984).
- [36] G. Giacomin, *Random Polymer Models* (Imperial College Press, London, 2007).
- [37] *Theory of Helix-Coil Transition in Biopolymers*, edited by D. Poland and H. A. Scheraga (Academic Press, New York, 1970).
- [38] M. Fisher, *J. Chem. Phys.* **45**, 1469 (1966).
- [39] M. S. Causo, B. Coluzzi, and P. Grassberger, *Phys. Rev. E* **62**, 3958 (2000).
- [40] E. Carlon, E. Orlandini, and A. L. Stella, *Phys. Rev. Lett.* **88**, 198101 (2002); M. Baiesi, E. Carlon, and A. L. Stella, *Phys. Rev. E* **66**, 021804 (2002); M. Baiesi, E. Carlon, Y. Kafri, D. Mukamel, E. Orlandini, and A. L. Stella, *ibid.* **67**, 021911 (2002).
- [41] Y. Kafri, D. Mukamel, and L. Peliti, *Phys. Rev. Lett.* **85**, 4988 (2000); *Eur. Phys. J. B* **27**, 135 (2002).
- [42] G. Forgacs, J. M. Luck, Th. M. Nieuwenhuizen, and H. Orland, *Phys. Rev. Lett.* **57**, 2184 (1986); *J. Stat. Phys.* **51**, 29 (1988).
- [43] B. Derrida, V. Hakim, and J. Vannimenus, *J. Stat. Phys.* **66**, 1189 (1992).
- [44] S. M. Bhattacharjee and S. Mukherji, *Phys. Rev. Lett.* **70**, 49 (1993); S. Mukherji and S. M. Bhattacharjee, *Phys. Rev. E* **48**,

- 3483 (1993).
- [45] H. Kallabis and M. Lässig, Phys. Rev. Lett. **75**, 1578 (1995).
- [46] D. Cule and T. Hwa, Phys. Rev. Lett. **79**, 2375 (1997).
- [47] L.-H. Tang and H. Chaté, Phys. Rev. Lett. **86**, 830 (2001).
- [48] T. Garel and C. Monthus, Eur. Phys. J. B **46**, 117 (2005).
- [49] C. Monthus and T. Garel, Eur. Phys. J. B **48**, 393 (2005).
- [50] A. Chhabra and R. V. Jensen, Phys. Rev. Lett. **62**, 1327 (1989).
- [51] R. B. Griffiths, Phys. Rev. Lett. **23**, 17 (1969); A. B. Harris, Phys. Rev. B **12**, 203 (1975); A. J. Bray, Phys. Rev. Lett. **59**, 586 (1987); T. Vojta, J. Phys. A **39**, R143 (2006).